Geophysical Research Letters

RESEARCH LETTER
10.1029/2022GL100011

Key Points:

- The patterns of observed sea-surface temperature and sea-level pressure trends differ significantly from CMIP5/6 historical simulations
- The rate of Indo-Pacific Warm Pool warming relative to tropical-mean warming is particularly anomalous in observations compared to models
- Patterns of observed changes that climate models do not reproduce are isolated with a signal-to-noise maximizing pattern analysis

Supporting Information:

Supporting Information may be found in the online version of this article.

Correspondence to:

R. C. J. Wills,
rcwills@uw.edu

Citation:

Wills, R. C. J., Dong, Y., Proistosecu, C., Armour, K. C., & Battisti, D. S. (2022). Systematic climate model biases in the large-scale patterns of recent sea-surface temperature and sea-level pressure change. *Geophysical Research Letters*, *49*, e2022GL100011. https://doi.org/10.1029/2022GL100011

Received 14 JUN 2022
Accepted 24 AUG 2022

Systematic Climate Model Biases in the Large-Scale Patterns of Recent Sea-Surface Temperature and Sea-Level Pressure Change

Robert C. J. Wills[1], Yue Dong[2], Cristian Proistosecu[3], Kyle C. Armour[1,4], and David S. Battisti[1]

[1]Department of Atmospheric Sciences, University of Washington, Seattle, WA, USA, [2]Lamont-Doherty Earth Observatory, Columbia University, Palisades, NY, USA, [3]Department of Atmospheric Sciences, University of Illinois Urbana-Champaign, Champaign, IL, USA, [4]School of Oceanography, University of Washington, Seattle, WA, USA

Abstract Observed surface temperature trends over recent decades are characterized by (a) intensified warming in the Indo-Pacific Warm Pool and slight cooling in the eastern equatorial Pacific, consistent with Walker circulation strengthening, and (b) Southern Ocean cooling. In contrast, state-of-the-art coupled climate models generally project enhanced warming in the eastern equatorial Pacific, Walker circulation weakening, and Southern Ocean warming. Here we investigate the ability of 16 climate model large ensembles to reproduce observed sea-surface temperature and sea-level pressure trends over 1979–2020 through a combination of externally forced climate change and internal variability. We find large-scale differences between observed and modeled trends that are very unlikely (<5% probability) to occur due to internal variability as represented in models. Disparate trends in the ratio of Indo-Pacific Warm Pool to tropical-mean warming, which shows little multi-decadal variability in models, hint that model biases in the response to historical forcing constitute part of the discrepancy.

Plain Language Summary Regional climate change depends not only on the magnitude of global warming, but also on the spatial pattern of warming. We show that the spatial pattern of observed surface temperature changes since 1979 is highly unusual, and many aspects of it cannot be reproduced in current climate models, even when accounting for the influence of natural variability. We find a particularly large discrepancy in the rate of warming within the western Pacific Ocean and eastern Indian Ocean, which suggests that models have systematic biases in the response of sea-surface temperature patterns to anthropogenic forcing, because the contribution of natural variability to multi-decadal trends is thought to be relatively small in this region. Our work raises the possibility that the recent trends toward more La-Niña-like conditions may be partly a response to anthropogenic forcing, even though most existing climate model and paleoclimate evidence suggests that trends will eventually reverse toward more El-Niño-like conditions, with an associated shift in regional climate trends.

1. Introduction

Earth's climatological pattern of sea-surface temperature (SST) plays a key role in shaping the large-scale atmospheric circulation and regional climate. In particular, the relative warmth of the Warm Pool in the western Indo-Pacific compared to the Cold Tongue in the eastern equatorial Pacific drives the Walker circulation in the tropical atmosphere, which through its impact on the upper tropospheric divergence in the Warm Pool generates large-scale atmospheric Rossby waves that propagate into higher latitudes and impact climate around the globe (Bjerknes, 1969; Sardeshmukh & Hoskins, 1988). This is part of a two-way coupling between the tropical atmosphere and ocean; the Walker circulation also helps shape the climatological SST pattern by driving upwelling of cold waters in the Cold Tongue and ocean heat-flux convergence in the Warm Pool (Bjerknes, 1969; Neelin et al., 1998).

In response to anthropogenic greenhouse gas forcing, climate models generally show weakening of the Walker circulation (Vecchi et al., 2006) and enhanced warming in the eastern equatorial Pacific (Meehl & Washington, 1996). In contrast, SST observations show enhanced warming in the Indo-Pacific Warm Pool and weak cooling in the eastern equatorial Pacific over the 20th century (Cane et al., 1997; Coats & Karnauskas, 2017; Karnauskas et al., 2009; Solomon & Newman, 2012) as well as a pronounced strengthening of the tropical Pacific zonal SST gradient since the mid 1970s (Watanabe et al., 2021; Wills et al., 2020). Sea-level pressure

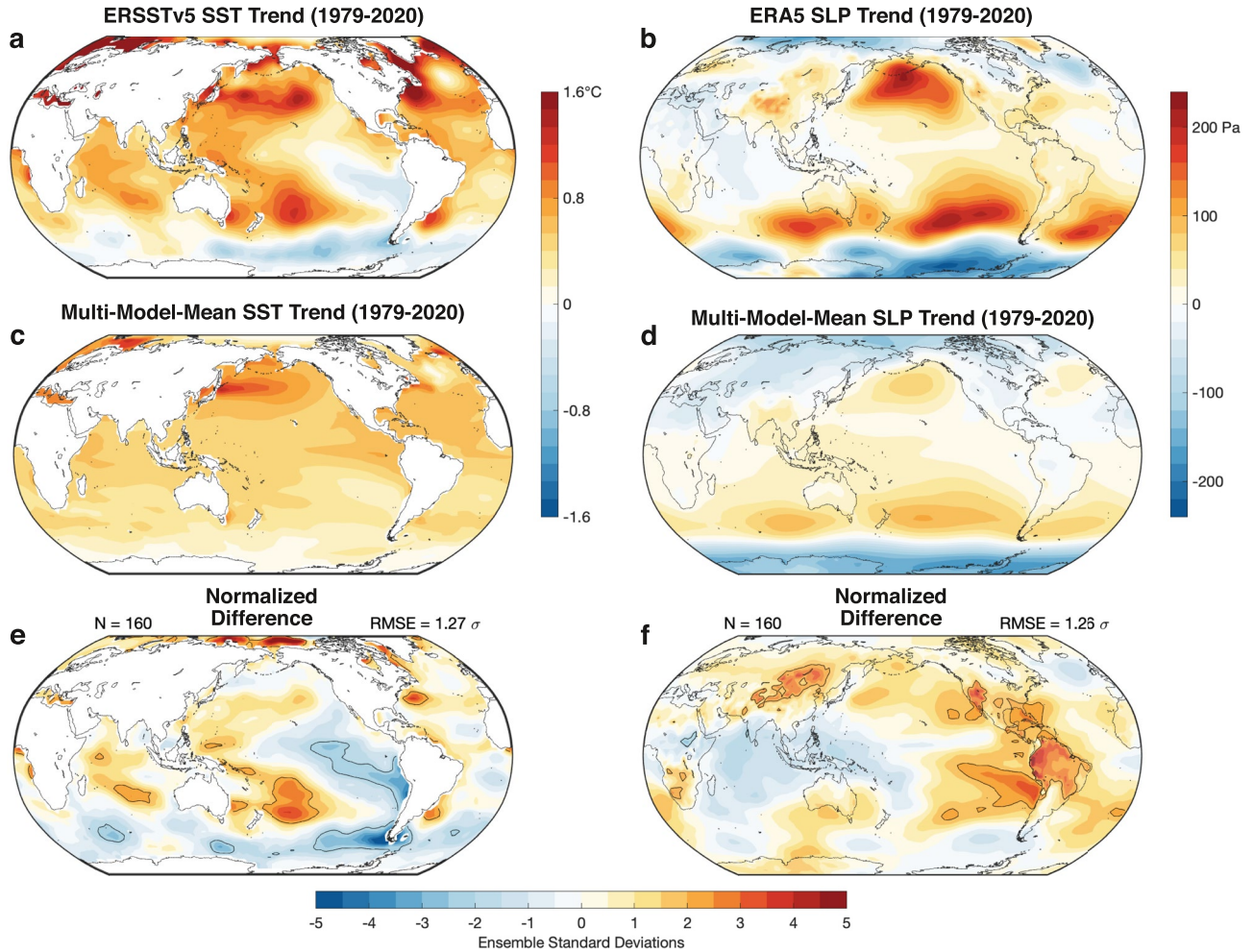

Figure 1. Observed trends (per 41 yr) in annual-mean (a) sea-surface temperature (SST) and (b) sea-level pressure (SLP) over 1979–2020 from Extended Reconstructed SST data set v5 (ERSSTv5) (Huang et al., 2017) and the ERA5 reanalysis (Hersbach et al., 2020), respectively. Modeled trends in (c) SST and (d) SLP over 1979–2020, from the multi-model mean of simulations with 16 climate model large ensembles (LEs) (Table 1). The SST trends in each LE have been rescaled such that their global mean matches that in ERSSTv5. Observed trends in (e) SST and (f) SLP over 1979–2020, expressed in ensemble standard deviations away from the multi-model mean (i.e., the difference in trends between observations and the multi-model mean divided by the square root of the average variance in trends within LEs). Panels (c–f) are computed with the first 10 members of each LE such that models are weighted equally. The ±2 standard deviation contour is shown with a black line. The root mean square error over 60°S–60°N of the maps in panels (e and f) are shown in the upper right.

(SLP) observations show weakening of the Walker circulation over the 20th century (Tokinaga et al., 2012; Vecchi et al., 2006), however, the Walker circulation has strengthened since 1979 (Chung et al., 2019; Kociuba & Power, 2015; L'Heureux et al., 2013; Ma & Zhou, 2016; Zhao & Allen, 2019), in contrast to fully coupled historical simulations of this period (Figure 1). Recent decades have also been characterized by Southern Ocean cooling and sea-ice expansion, in contrast to the anthropogenically forced changes simulated in climate models (Fan et al., 2014; Turner & Overland, 2009).

It remains an open question whether the differences in recent multi-decadal trends between observations and models resulted from anomalous multi-decadal variability or from aspects of the forced climate response not captured by models. Some studies suggest that these difference in Pacific and Southern Ocean trends could have resulted from internal atmosphere-ocean variability (Chung et al., 2019, 2022; Olonscheck et al., 2020; Watanabe et al., 2021; L. Zhang et al., 2019; Zhao & Allen, 2019), while others suggest they result in part from missing forcings or model biases in the pattern of response to forcing (Bintanja et al., 2013; Coats & Karnauskas, 2018; Kohyama et al., 2017; Kostov et al., 2018; Schneider & Deser, 2018; Seager et al., 2019, 2022; Suarez-Gutierrez et al., 2021; Wills et al., 2020). It is critical to distinguish between these hypotheses in order to predict future SST trends and the associated atmospheric circulation changes.

Table 1
CMIP5 and CMIP6 Large Ensembles Covering the Period 1979–2020, the Scenarios Used, and the Number of Ensemble Members Used (N)

Model	Scenarios	*N*	Reference
CESM1.1	Historical, RCP8.5	40	Kay et al. (2015)
CanESM2	Historical, RCP8.5	50	Kirchmeier-Young et al. (2017)
CSIRO-Mk3.6	Historical, RCP8.5	30	Jeffrey et al. (2013)
GFDL-CM3	Historical, RCP8.5	20	Sun et al. (2018)
GFDL-ESM2M	Historical, RCP8.5	30	Rodgers et al. (2015)
MPI-ESM	Historical, RCP8.5	100	Maher et al. (2019)
ACCESS-ESM1.5	Historical, SSP2-4.5	13	Ziehn et al. (2020)
CanESM5	Historical, SSP3-7.0	25	Swart et al. (2019)
CESM2.1	Historical, SSP3-7.0	99	Rodgers et al. (2021)
CNRM-CM6.1	Historical, SSP2-4.5	10	Voldoire et al. (2019)
EC-Earth3	Historical, SSP5-8.5	50	Wyser et al. (2021)
GISS-E2.1-G	Historical, SSP3-7.0	10	Kelley et al. (2020)
IPSL-CM6A-LR	Historical, SSP3-7.0	11	Boucher et al. (2020)
MIROC6	Historical, SSP5-8.5	50	Tatebe et al. (2019)
MIROC-ES2L	Historical, SSP2-4.5	30	Hajima et al. (2020)
NorCPM1	Historical, SSP2-4.5	30	Bethke et al. (2021)

Note. The experimental setups and forcing scenarios for the CMIP5 (top) and CMIP6 simulations (bottom) are described in Taylor et al. (2012) and Eyring et al. (2016), respectively.

Here, we leverage a recent proliferation of climate model data from initial-condition large ensembles (LEs) (Deser, Lehner, et al., 2020) to evaluate which aspects of the mismatch between observed and modeled trends can be explained by internal multi-decadal variability. In initial-condition LEs, the same model is run multiple times with the same forcing but small differences in the initial condition, such that each ensemble member shows a different realization of internal variability. The ensemble mean thus shows the forced climate response, while the ensemble spread shows the range of possible realizations due to internal variability. Olonscheck et al. (2020) used LEs to show that local 30-yr SST trends in climate models are largely consistent with observations, when accounting for internal variability. However, several other recent studies (Seager et al., 2019, 2022; Watanabe et al., 2021) have shown discrepancies between observations and models in longer-term equatorial Pacific SST trends. In this study, we will evaluate the large-scale pattern of SST and SLP changes during the well-observed 42-yr period since 1979, during which the Walker circulation and Pacific zonal SST gradient trends are particularly anomalous, and will show that the discrepancies in equatorial Pacific trends over this period are part of a large-scale pattern of systematic biases in trends between climate models and observations.

2. Climate Model Large Ensembles Unable to Reproduce Observed Trends

We analyze annual-mean SST and SLP in simulations from 16 climate models that have at least 10 ensemble members for the period 1979–2020 under historical and future forcing scenarios (Table 1). Historical simulations only extend to 2005 (CMIP5) or 2014 (CMIP6), and different ensembles use different scenarios afterward, namely RCP8.5, SSP2-4.5, SSP3-7.0, and SSP5-8.5, but differences between these scenarios are small through the year 2020. We compare modeled trends against observational SST data from the Extended Reconstructed SST data set v5 (ERSSTv5) (Huang et al., 2017), the COBE SST data set (Ishii et al., 2005), and the Atmospheric Model Intecomparison Project SST boundary condition data set (Hurrell et al., 2008), and SLP data from the ERA5 (Hersbach et al., 2020) and JRA55 (Kobayashi et al., 2015) reanalyzes. All model output and observational data are linearly interpolated to a common 1.5° analysis grid used by the ETH Zurich CMIP6 next-generation archive (Brunner et al., 2020).

The multi-model-mean SST trends over 1979–2020 (Figure 1c) are relatively spatially uniform except for enhanced warming in the North Pacific and muted warming in the North Atlantic warming hole and the Southern

Ocean. Compared to the multi-model mean, observed SST trends (Figure 1a) show much larger warming in the northwest Atlantic and southwest Pacific, cooling instead of warming in the Southern Ocean (Figure 2c), and opposite trends in the Pacific zonal SST gradient (Figure 2a). In this comparison of modeled and observed SST trends, we have rescaled the ensemble-mean SST trends in each model such that the global-mean SST trend matches that in ERSSTv5 over 1979–2020, removing differences in global-mean warming rate between models (due largely to differences in climate sensitivity) and focusing instead on differences in the pattern of SST trends. This rescaling removes a global-mean SST trend difference between models and observations due to climate models overestimating recent warming (Jiménez-de-la Cuesta & Mauritsen, 2019; Nijsse et al., 2020; Tokarska et al., 2020).

The SLP trends over 1979–2020 in ERA5 reanalysis (Figure 1b) and models (Figure 1d) both show positive (anticyclonic) trends in the midlatitude oceans and negative (cyclonic) trends in the high latitudes, but the trends in the midlatitude oceans are much larger in observations than in models, and observations show a strengthening of the Walker circulation, as measured by the zonal SLP gradient across the equatorial Pacific, which is not seen in the multi-model mean (Figure 2c). Global-mean SLP trends are retained in the analysis, because absolute surface pressure is assimilated in ERA5. There is a global-mean SLP trend of 20.6 Pa (41 yr)$^{-1}$ in ERA5, compared to −0.3 Pa (41 yr)$^{-1}$ in the multi-model mean, potentially related to the lack of mass conservation in the reanalysis. Removing the global-mean SLP trend would serve to shift the observed trends toward more negative values, while preserving the range of values.

To analyze how internal variability could have contributed to the differences in trends between observations and models, we calculate where the observations lie within the distribution of trends simulated by the LEs (Figures 1e and 1f). To do so, we divide the difference in trends (observations minus multi-model mean) by the multi-model ensemble standard deviation (i.e., the square root of the multi-model mean of the ensemble variance at each grid point). If the observations were consistent with the forced response and internal variability as represented in the models, and the distribution of anomalies due to internal variability is well-described by a Gaussian, then there would only be a ∼5% probability of observing a normalized difference more extreme than ±2 ensemble standard deviations. However, differences larger than this are found in many regions (12% of the globe for SST; 8% for SLP), including the strong observed warming in the Indian Ocean, West Pacific, South Pacific Convergence Zone, and Gulf Stream, the observed cooling in the Southern Ocean and southeast Pacific, and the observed SLP increase in the eastern Pacific, the Caribbean, South America, and the Mongolian Plateau (note however that SLP over topography is sensitive to the surface air temperature used in the adjustment to mean sea level). Differences in trends (from the multi-model mean) this large are very unlikely (<5% probability) to occur within the models.

The same basic patterns of normalized trend differences can be found by comparing observations to each LE separately (Figures S1 and S2 in Supporting Information S1) or when using different observational products (Figure S3 in Supporting Information S1). CESM2 and MPI-ESM show the smallest discrepancies with observations in the tropics (Figures S1 and S2 in Supporting Information S1), owing in part to strong (but potentially unrealistic; Samanta et al. (2018)) tropical Pacific multi-decadal variability in these models (Figures 2a, 2b, and 2d). A similar pattern of SST trend differences can be found in both boreal winter and boreal summer (Figures S4 and S5 in Supporting Information S1), though SST trends in the South Pacific are more anomalous in austral winter. The pattern of SLP trend differences differs between boreal winter and boreal summer (Figures S4 and S5 in Supporting Information S1), but both seasons show anomalous Walker circulation strengthening compared to the multi-model mean. Observed trends over a longer time period (1958–2021) are even more anomalous on average compared to the trends simulated by the LEs (Figure S6 in Supporting Information S1), though trends in Southern Ocean SST and Walker circulation strength are more consistent with models over this period.

The unusual nature of the observed trends compared to what is possible in coupled climate models is also apparent in a number of key climate indices including the Pacific zonal SST gradient (Figure 2a), the Walker circulation strength (Figure 2d), and Southern Ocean SST (Figure 2c). No ensemble member simulates the magnitudes of both Pacific SST gradient strengthening and Southern Ocean cooling found in ERSSTv5. The relative rate of Indo-Pacific Warm Pool warming (per degree of tropical-mean SST change), which plays a key role in global radiative feedbacks (Dong et al., 2019), is also particularly anomalous (Figure 2b), with most models showing trends of near 1°C (°C)$^{-1}$ (i.e., Warm Pool warming rate equal to the tropical average), whereas observations show trends of around 1.3°C (°C)$^{-1}$, which are only reproduced in a few ensemble members of one model (CESM2). Previous studies have also reported anomalous observed trends in related metrics such as the warming

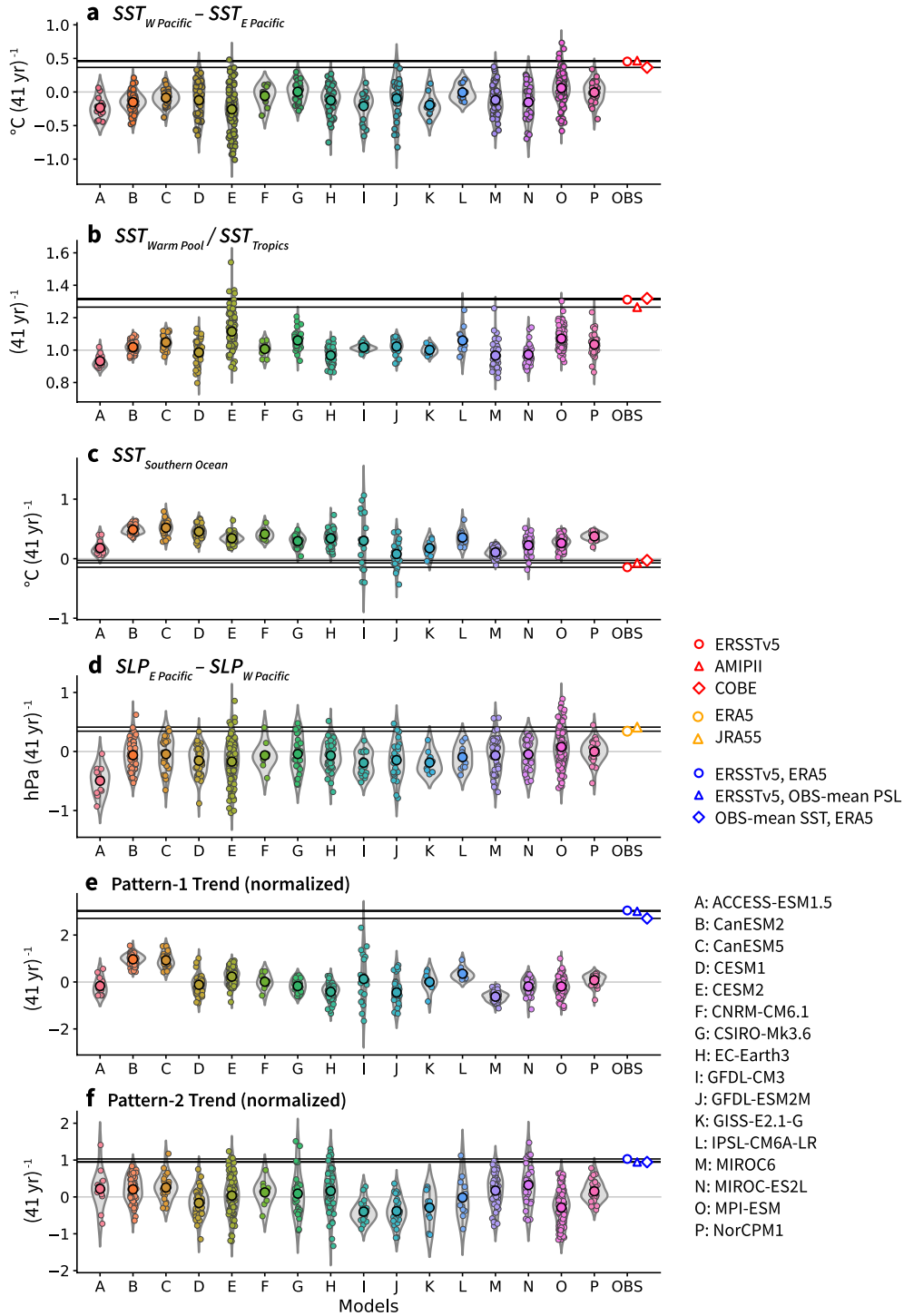

Figure 2. Comparison of observed trends (1979–2020) in key indices with those in all ensemble members from 16 large ensembles: (a) the Pacific sea-surface temperature (SST) gradient index used in Watanabe et al. (2021), defined as the difference between the western equatorial Pacific (5°S–5°N, 110°E–180°) and eastern equatorial Pacific (5°S–5°N, 180°–80°W); (b) the ratio of Indo-Pacific Warm Pool (30°S–30°N, 50°E–160°W) SST warming to tropical-mean (30°S–30°N) SST warming; (c) Southern Ocean SST (45°S–75°S); (d) Walker Circulation strength, defined as in Vecchi et al. (2006) as the difference in sea-level pressure between the eastern equatorial Pacific (5°S–5°N, 160°W–80°W) and western equatorial Pacific (5°S–5°N, 80°E–160°E); (e and f) the signal-to-noise maximizing pattern indices shown in Figure 3. Violin plots (Waskom, 2021) for each model can be compared with multiple observational products, shown on the right-hand side. Ensemble average trends for each index and model are shown with black circles. See Figure S7 in Supporting Information S1 for a map of the averaging regions.

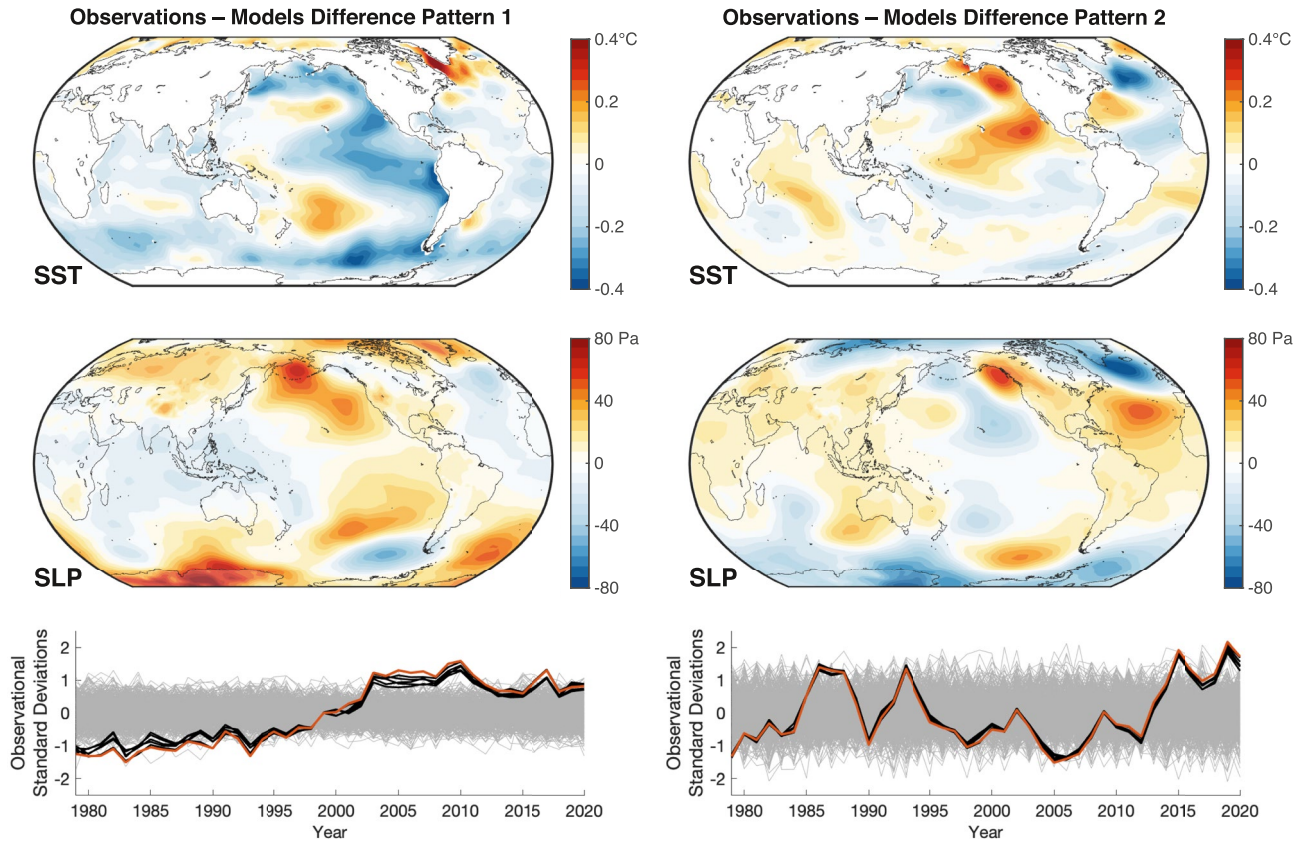

Figure 3. First and second multi-field (sea-surface temperature [SST] and sea-level pressure [SLP]) signal-to-noise maximizing patterns, from an analysis that maximizes the ratio of signal to noise in the leading patterns, where signal is defined as the difference between observations and the multi-model mean on 5-yr and longer timescales and noise consists of inter-model differences, inter-ensemble-member differences, and sub-5-yr variability, with 20 EOFs included in the analysis (see Figure S9 in Supporting Information S1 for the sensitivity to the number of EOFs included). The orange (black) lines show the amplitude of anomalies in these patterns in ERSSTv5/ERA5 (and other combinations of observational products) relative to the multi-model mean. The gray lines show the amplitude of these patterns in each member of the multi-model large ensemble relative to the multi-model mean. Normalization is such that the orange line has unit standard deviation and the SST/SLP pattern shows the anomalies associated with a 1-standard-deviation anomaly in the associated index.

in tropical convective regions (Fueglistaler & Silvers, 2021) or the tropical inter-basin warming contrast (Zhang & Karnauskas, 2017). There are also large discrepancies between observed and modeled SST trends in the southwest Pacific (Figure S8 in Supporting Information S1), where observed SST trends have been linked to Southern Hemisphere SLP trends and an ongoing drought in Chile (Garreaud et al., 2019, 2021).

3. Isolating the Observed Pattern of Change Not Reproduced in Models

To isolate the time varying SST and SLP anomalies contributing to the discrepancy between modeled and observed trends, we use a signal-to-noise maximizing pattern analysis (Déqué, 1988; Schneider & Griffies, 1999; Ting et al., 2009; Wills et al., 2020). Our goal is to identify the aspects of observed SST and SLP variability and trends over 1979–2020 that are not captured by any of the simulations in the multi-model LE. In this way, we can highlight aspects of the observed trends that are least consistent with the variability and change simulated by models.

First, we generate a difference ensemble, where each member is composed of the difference between observations and an individual member of one of the LEs, with 10 ensemble members used from each model (160 members total). The ensemble mean of the difference ensemble is thus the difference between observations and the multi-model mean, and the ensemble variance arises from inter-model and inter-ensemble-member differences within the multi-model LE. Next, we solve for patterns with the maximum signal-to-noise ratio (SNR), where signal is defined as the difference between observations and the multi-model mean on 5-yr and longer timescales, and noise is defined as all other variance in the difference ensemble (i.e., due to inter-model differences,

inter-ensemble-member differences, and sub-5-yr variability). We use a 5-yr Lanczos lowpass filter in defining the signal to focus on low-frequency differences between observations and models that could contribute to the multi-decadal-trend difference. Unlike in the analysis for Figure 1, we do not rescale SST to account for differences in global-mean warming rate between models, because this would also modify the amplitude of internal variability. SST and SLP are normalized by their total variance such that they are weighted equally in the analysis.

The leading SST/SLP pattern shows less warming than models in a triangular region in the eastern tropical and subtropical Pacific, the Pacific sector of the Southern Ocean, and the subpolar North Pacific; more warming than models in the Labrador and Irminger Seas and the southwest Pacific; strengthening of the Walker Circulation and weakening of the Aleutian Low compared to models; and anomalies associated with the Pacific-South American pattern (Figure 3). The anomaly patterns are similar to those in Figures 1e and 1f but are expressed in absolute units instead of ensemble standard deviations. They therefore show the actual magnitude of anomalies (compared to the multi-model mean) that occurred in the observational data. This SST/SLP pattern increased monotonically from 1979 through 2003, then has shown relatively little change since 2003 (Figure 3). Despite the lack of changes in this pattern since 2003, its trend over the full time-period is still highly anomalous compared to trends in this pattern in models (Figure 2e), and none of the 598 ensemble members show the magnitude of trend found in observations. Only one ensemble member of one model (GFDL-CM3) shows anything close to the observed trends, owing to the large amplitude of Southern Ocean multi-decadal variability in versions of the GFDL model (Wills et al., 2021; L. Zhang et al., 2017), which projects strongly onto this pattern.

The second SST/SLP pattern is focused in the North Pacific and North Atlantic, potentially showing observations-model differences in the internal variability in these regions (Figure 3). The associated SLP anomalies capture an observed trend toward positive anomalies in the North Atlantic Oscillation, as well as the development of an anomalous ridge over the northeast Pacific (Swain et al., 2014). Together, the midlatitude SST and SLP anomaly patterns are consistent with a response of upper-ocean temperature anomalies to atmospheric anomalies (Battisti et al., 2019). The time evolution of this SST/SLP pattern shows decadal variability, a trend over the full time-period with a magnitude greater than that in most ensemble members (Figure 2f), and a particularly anomalous trend since 2005. This pattern thus shows how observed decadal variability differs from that in models, as well as including part of the observations-models difference in the monotonic trend over 1979–2020. Interestingly, the model that is closest to reproducing the trend in pattern 1 (GFDL-CM3) is furthest from reproducing the trend in pattern 2 (Figure 2).

The signal-to-noise maximizing analysis used here is designed to identify patterns that are highly anomalous in observations compared to models, so a question naturally arises regarding the extent to which it is guaranteed to find something even if the models were capable of reproducing observations given enough realizations. To address this, we repeat this analysis on difference ensembles sampling inter-model differences and internal variability within the multi-model LE (Supporting Information S1). We find that anomaly patterns with as high a SNR as that for pattern 1 in Figure 3 commonly occur due to a combination of inter-model differences and internal variability within the LEs, but are unlikely (<12.5% chance) to occur due to internal variability alone (Figure S10 in Supporting Information S1). Even when patterns this anomalous do occur, they are different patterns than found for the difference between observations and models, and they rarely show such large trends over the full time period (<4% chance for internal variability alone).

4. Summary and Discussion

We have shown that observed SST and SLP trends over 1979–2020 are highly anomalous in several regions (Figure 1) and indices (Figure 2) compared to those simulated within a multi-model LE through a combination of forced responses and internal variability. The anomalous trends over 1979–2020 can be encapsulated in large-scale SST and SLP patterns that have trends that are undoubtedly outside the range of what can be simulated in climate models (Figures 2e, 2f, and 3). Our results illustrate that there are systematic climate model biases in the large-scale pattern of multi-decadal SST and SLP trends, even though climate models can reproduce observed SST trends over shorter time periods (Olonscheck et al., 2020) and in some tropical climate indices with large amounts of internal variability (Chung et al., 2019; Coats & Karnauskas, 2017; Watanabe et al., 2021; Figures 2a and 2d). While biased trends have been previously identified in the equatorial Pacific (Seager et al., 2019, 2022), our work shows that biased trends are a much more widespread problem in climate models.

4.1. Possible Interpretations

With only a single realization of the real climate system, it remains difficult to robustly identify the forced response in observations. Therefore, the identified trend differences could result either from systematic model biases in the response to historical forcing (e.g., Seager et al. (2019)) or from model biases in the amplitude or pattern of multi-decadal variability (e.g., Laepple and Huybers (2014)).

Many previous studies have invoked negative trends in the Pacific Decadal Oscillation (PDO) as an explanation for the anomalous pattern of trends in observations (e.g., Trenberth and Fasullo (2013); Chung et al. (2019)). However, with a return toward positive PDO conditions between 2013 and 2020, trends are no longer as anomalous in the North Pacific, while they remain anomalous in the South Pacific (Figure 1e), suggesting that the PDO is not the primary driver of the trend discrepancy for the full 1979–2020 period.

It has also been suggested that observed trends in the Southern Ocean could result from an anomalous phase of Southern Ocean multi-decadal variability (e.g., L. Zhang et al. (2019)). This remains plausible, though its relevance for lower latitude SST trends depends on an active body of work to quantify the teleconnections from Southern Ocean SST changes (Dong et al., 2022; Hwang et al., 2017; Kang et al., 2019; Kim et al., 2022; X. Zhang et al., 2021). Furthermore, there are several mechanisms for how recent Southern Ocean cooling and sea ice expansion could result from anthropogenic forcing, including wind shifts due to a combination of greenhouse gas and ozone forcing (Kostov et al., 2018; Thompson et al., 2011) and increased surface stratification resulting from precipitation changes and/or ice-sheet melt (Bintanja et al., 2013; De Lavergne et al., 2014; Pauling et al., 2016; Purich et al., 2018), the latter of which is not included in CMIP models. Specifying observed extratropical winds or adding Antarctic meltwater forcing to a climate model both shift the SST trend pattern closer to observations (Dong et al., 2022), but discrepancies in winds or meltwater forcing could result from a biased/missing forced response or from multi-decadal variability, so the ultimate cause of the observed Southern Ocean cooling trend remains an open question.

The large difference in the relative Warm Pool warming rate between models and observations (Figure 2b) is particularly hard to explain with internal variability. CMIP models show little multi-decadal variability in Warm Pool SST (Parsons et al., 2020), because strong global radiative damping to space in response to surface warming in convective regions precludes persistent SST anomalies without either large global energy budget anomalies or compensating feedbacks in other regions (Wills et al., 2021). A bias in the response of the tropical Pacific to historical forcing could result from climatological biases that make the eastern equatorial Pacific too sensitive to greenhouse gas forcing (Seager et al., 2019, 2022) and overwhelm the cooling influence of ocean upwelling (Clement et al., 1996), model biases in the response to geographic changes in aerosol optical depth (Deser, Phillips, et al., 2020; Heede & Fedorov, 2021; Qin et al., 2020; Shi et al., 2022; Smith et al., 2016), or remote influences of biases in the North Atlantic (McGregor et al., 2018) or Southern Ocean (discussed in the previous paragraph). Another possibility is that multi-decadal variability of tropical and subtropical SSTs is much too weak in models, as suggested by a comparison to paleoclimate proxies (Laepple & Huybers, 2014). Further, we hypothesize that the damping feedbacks in response to Warm Pool warming could be too efficient in models due to the tendency of parameterized convection to overstabilize convective regions (Holloway et al., 2012; Keil et al., 2021; Sohn et al., 2016), which would reduce both the modeled warming rate and the modeled amplitude of multi-decadal variability in this region.

Building on methods to isolate the forced response in observations (Wills et al., 2020), our analysis in Figure 3 identifies the anomaly patterns that distinguish models and observations on long timescales, in an attempt to detect the difference in forced response between models and observations from amongst the noise of internal variability. There presumably remains an unquantifiable contribution of multi-decadal variability to these anomaly patterns. However, the large magnitude of multi-decadal trends in these patterns compared to what is found in CMIP5/6 models, together with the projection of pattern 1 onto the ratio of Indo-Pacific Warm Pool to tropical-mean warming, which shows little multi-decadal variability in models, lead us to conclude that it is extremely unlikely that this pattern of trend discrepancies results entirely from internal variability. Our analysis provides a starting point for more detailed mechanistic analysis to understand where model biases in the forced response are contributing.

4.2. Implications for Future Trends

Regardless of whether the differences in observed and modeled trends results from internal variability or from biases in the response to historical forcing, modeling and paleoclimate studies (Armour et al., 2016; Fedorov

et al., 2015; Forster et al., 2021; Heede & Fedorov, 2021; Tierney et al., 2019) suggest the East Pacific and Southern Oceans will eventually warm. Eventual warming in these regions favors more positive radiative feedbacks, which would lead to a higher effective climate sensitivity in the future compared to that inferred from historical observations (Andrews et al., 2018; Dong et al., 2021; Zhou et al., 2016). That observations have shown less warming in these regions than almost any model suggests that the so-called pattern effect on climate sensitivity, due to changing SST patterns, could be larger in the real world than in models. A future shift toward a warming pattern with more warming in the eastern equatorial Pacific would also lead to major changes in the Walker circulation and the associated large-scale circulation and precipitation patterns. Without understanding why large-scale SST and SLP trends are so anomalous over the recent observational period or when and by how much delayed warming regions in the East Pacific and Southern Oceans will warm, we are left with a huge source of uncertainty in multi-decadal projections of regional and global climate.

Data Availability Statement

CMIP5 LE data were obtained from the U.S. CLIVAR Multi-Model Large Ensemble Archive, which can be downloaded following instructions at https://www.cesm.ucar.edu/projects/community-projects/MMLEA/. CMIP6 LE data were obtained from the ETH Zurich CMIP6 next-generation archive (Brunner et al., 2020). CESM2 LE data were obtained from the National Center for Atmospheric Research following instructions at https://www.cesm.ucar.edu/projects/community-projects/LENS2/data-sets.html. All observational data are publicly available. ERSSTv5 and COBE SST data were obtained from NOAA/OAR/ESRL PSL (https://psl.noaa.gov/data/gridded/data.noaa.ersst.v5.html; https://psl.noaa.gov/data/gridded/data.cobe.html). ERA5 data were obtained from the Copernicus Climate Data Store (https://cds.climate.copernicus.eu/#!/search?text=ERA5%20monthly%20single%20levels&type=dataset). JRA55 data were obtained from the NCAR Research Data Archive (https://rda.ucar.edu/datasets/ds628.1/). Code and preprocessed data used for the analysis in this paper is available at https://doi.org/10.5281/zenodo.6998934.

Acknowledgments

R. C. J. W and D. S. B. were supported by the National Science Foundation grants AGS-1929775 and AGS-2203543. R. C. J. W., C. P., and K. C. A. were supported by National Oceanic and Atmospheric Administration MAPP Program Award NA20OAR4310391. Y. D. was supported by the NOAA Climate and Global Change Postdoctoral Fellowship Program, administered by UCAR's Cooperative Programs for the Advancement of Earth System Science (CPAESS) under award NA21OAR4310383. Y. D. and K. C. A. were supported by National Science Foundation Grant AGS-1752796. K. C. A. was supported by an Alfred P. Sloan Research Fellowship (Grant No. FG-2020-13568).

References

Andrews, T., Gregory, J. M., Paynter, D., Silvers, L. G., Zhou, C., Mauritsen, T., et al. (2018). Accounting for changing temperature patterns increases historical estimates of climate sensitivity. *Geophysical Research Letters*, *45*(16), 8490–8499. https://doi.org/10.1029/2018gl078887

Armour, K. C., Marshall, J., Scott, J. R., Donohoe, A., & Newsom, E. R. (2016). Southern Ocean warming delayed by circumpolar upwelling and equatorward transport. *Nature Geoscience*, *9*(7), 549–554. https://doi.org/10.1038/ngeo2731

Battisti, D. S., Vimont, D. J., & Kirtman, B. P. (2019). 100 years of progress in understanding the dynamics of coupled atmosphere–ocean variability. *Meteorological Monographs*, *59*, 8.1–8.57. https://doi.org/10.1175/amsmonographs-d-18-0025.1

Bethke, I., Wang, Y., Counillon, F., Keenlyside, N., Kimmritz, M., Fransner, F., et al. (2021). NorCPM1 and its contribution to CMIP6 DCPP. *Geoscientific Model Development*, *14*(11), 7073–7116. https://doi.org/10.5194/gmd-14-7073-2021

Bintanja, R., van Oldenborgh, G. J., Drijfhout, S., Wouters, B., & Katsman, C. (2013). Important role for ocean warming and increased ice-shelf melt in Antarctic sea-ice expansion. *Nature Geoscience*, *6*(5), 376–379. https://doi.org/10.1038/ngeo1767

Bjerknes, J. (1969). Atmospheric teleconnections from the equatorial Pacific. *Monthly Weather Review*, *97*(3), 163–172. https://doi.org/10.1175/1520-0493(1969)097<0163:atftep>2.3.co;2

Boucher, O., Servonnat, J., Albright, A. L., Aumont, O., Balkanski, Y., Bastrikov, V., et al. (2020). Presentation and evaluation of the IPSL-CM6A-LR climate model. *Journal of Advances in Modeling Earth Systems*, *12*(7), e2019MS002010. https://doi.org/10.1029/2019MS002010

Brunner, L., Hauser, M., Lorenz, R., & Beyerle, U. (2020). *The ETH Zurich CMIP6 next generation archive: Technical documentation* (Vol. 10). ETH Zürich. https://doi.org/10.5281/zenodo.3734128

Cane, M. A., Clement, A. C., Kaplan, A., Kushnir, Y., Pozdnyakov, D., Seager, R., et al. (1997). Twentieth-century sea surface temperature trends. *Science*, *275*(5302), 957–960. https://doi.org/10.1126/science.275.5302.957

Chung, E.-S., Kim, S.-J., Timmermann, A., Ha, K.-J., Lee, S.-K., Stuecker, M. F., et al. (2022). Antarctic sea-ice expansion and Southern Ocean cooling linked to tropical variability. *Nature Climate Change*, *12*(5), 1–8. https://doi.org/10.1038/s41558-022-01339-z

Chung, E.-S., Timmermann, A., Soden, B. J., Ha, K.-J., Shi, L., & John, V. O. (2019). Reconciling opposing Walker circulation trends in observations and model projections. *Nature Climate Change*, *9*(5), 405–412. https://doi.org/10.1038/s41558-019-0446-4

Clement, A. C., Seager, R., Cane, M. A., & Zebiak, S. E. (1996). An ocean dynamical thermostat. *Journal of Climate*, *9*(9), 2190–2196. https://doi.org/10.1175/1520-0442(1996)009<2190:aodt>2.0.co;2

Coats, S., & Karnauskas, K. (2017). Are simulated and observed twentieth century tropical Pacific sea surface temperature trends significant relative to internal variability? *Geophysical Research Letters*, *44*(19), 9928–9937. https://doi.org/10.1002/2017gl074622

Coats, S., & Karnauskas, K. (2018). A role for the equatorial undercurrent in the ocean dynamical thermostat. *Journal of Climate*, *31*(16), 6245–6261. https://doi.org/10.1175/jcli-d-17-0513.1

De Lavergne, C., Palter, J. B., Galbraith, E. D., Bernardello, R., & Marinov, I. (2014). Cessation of deep convection in the open Southern Ocean under anthropogenic climate change. *Nature Climate Change*, *4*(4), 278–282. https://doi.org/10.1038/nclimate2132

Déqué, M. (1988). 10-day predictability of the Northern Hemisphere winter 500-mb height by the ECMWF operational model. *Tellus A*, *40*(1), 26–36. https://doi.org/10.1111/j.1600-0870.1988.tb00328.x

Deser, C., Lehner, F., Rodgers, K., Ault, T., Delworth, T., DiNezio, P., et al. (2020). Insights from Earth system model initial-condition large ensembles and future prospects. *Nature Climate Change*, *10*(4), 1–10. https://doi.org/10.1038/s41558-020-0731-2

Deser, C., Phillips, A. S., Simpson, I. R., Rosenbloom, N., Coleman, D., Lehner, F., et al. (2020). Isolating the evolving contributions of anthropogenic aerosols and greenhouse gases: A new CESM1 large ensemble community resource. *Journal of Climate*, *33*(18), 7835–7858. https://doi.org/10.1175/jcli-d-20-0123.1

Dong, Y., Armour, K. C., Battisti, D. S., & Blanchard-Wrigglesworth, E. (2022). Two-way teleconnections between the Southern Ocean and the tropical Pacific via a dynamic feedback. *Journal of Climate*, 1–37. in press. https://doi.org/10.1175/JCLI-D-22-0080.1

Dong, Y., Armour, K. C., Proistosescu, C., Andrews, T., Battisti, D. S., Forster, P. M., et al. (2021). Biased estimates of equilibrium climate sensitivity and transient climate response derived from historical CMIP6 simulations. *Geophysical Research Letters*, *48*(24), e2021GL095778. https://doi.org/10.1029/2021gl095778

Dong, Y., Proistosescu, C., Armour, K. C., & Battisti, D. S. (2019). Attributing historical and future evolution of radiative feedbacks to regional warming patterns using a Green's function approach: The preeminence of the western Pacific. *Journal of Climate*, *32*(17), 5471–5491. https://doi.org/10.1175/jcli-d-18-0843.1

Eyring, V., Bony, S., Meehl, G. A., Senior, C. A., Stevens, B., Stouffer, R. J., & Taylor, K. E. (2016). Overview of the Coupled Model Intercomparison Project Phase 6 (CMIP6) experimental design and organization. *Geoscientific Model Development*, *9*(5), 1937–1958. https://doi.org/10.5194/gmd-9-1937-2016

Fan, T., Deser, C., & Schneider, D. P. (2014). Recent Antarctic sea ice trends in the context of Southern Ocean surface climate variations since 1950. *Geophysical Research Letters*, *41*(7), 2419–2426. https://doi.org/10.1002/2014gl059239

Fedorov, A. V., Burls, N. J., Lawrence, K. T., & Peterson, L. C. (2015). Tightly linked zonal and meridional sea surface temperature gradients over the past five million years. *Nature Geoscience*, *8*(12), 975–980. https://doi.org/10.1038/ngeo2577

Forster, P., Storelvmo, T., Armour, K., Collins, W., Dufresne, J.-L., Frame, D., et al. (2021). The Earth's energy budget, climate feedbacks, and climate sensitivity. In *Climate change 2021: The physical science basis. contribution of working group I to the sixth assessment report of the intergovernmental panel on climate change* (pp. 923–1054). Cambridge University Press.

Fueglistaler, S., & Silvers, L. (2021). The peculiar trajectory of global warming. *Journal of Geophysical Research: Atmospheres*, *126*(4), e2020JD033629. https://doi.org/10.1029/2020jd033629

Garreaud, R. D., Boisier, J. P., Rondanelli, R., Montecinos, A., Sepúlveda, H. H., & Veloso-Aguila, D. (2019). The central Chile mega drought (2010–2018): A climate dynamics perspective. *International Journal of Climatology*, *40*(1), 421–439. https://doi.org/10.1002/joc.6219

Garreaud, R. D., Clem, K., & Veloso, J. V. (2021). The South Pacific pressure trend dipole and the southern blob. *Journal of Climate*, *34*(18), 7661–7676. https://doi.org/10.1175/jcli-d-20-0886.1

Hajima, T., Watanabe, M., Yamamoto, A., Tatebe, H., Noguchi, M. A., Abe, M., et al. (2020). Development of the MIROC-ES2L Earth system model and the evaluation of biogeochemical processes and feedbacks. *Geoscientific Model Development*, *13*(5), 2197–2244. https://doi.org/10.5194/gmd-13-2197-2020

Heede, U. K., & Fedorov, A. V. (2021). Eastern equatorial Pacific warming delayed by aerosols and thermostat response to CO_2 increase. *Nature Climate Change*, *11*(8), 696–703. https://doi.org/10.1038/s41558-021-01101-x

Hersbach, H., Bell, B., Berrisford, P., Hirahara, S., Horányi, A., Muñoz-Sabater, J., et al. (2020). The ERA5 global reanalysis. *Quarterly Journal of the Royal Meteorological Society*, *146*(730), 1999–2049. https://doi.org/10.1002/qj.3803

Holloway, C., Woolnough, S., & Lister, G. (2012). Precipitation distributions for explicit versus parametrized convection in a large-domain high-resolution tropical case study. *Quarterly Journal of the Royal Meteorological Society*, *138*(668), 1692–1708. https://doi.org/10.1002/qj.1903

Huang, B., Thorne, P. W., Banzon, V. F., Boyer, T., Chepurin, G., Lawrimore, J. H., et al. (2017). Extended reconstructed sea surface temperature, version 5 (ERSSTV5): Upgrades, validations, and intercomparisons. *Journal of Climate*, *30*(20), 8179–8205. https://doi.org/10.1175/jcli-d-16-0836.1

Hurrell, J. W., Hack, J. J., Shea, D., Caron, J. M., & Rosinski, J. (2008). A new sea surface temperature and sea ice boundary dataset for the Community Atmosphere Model. *Journal of Climate*, *21*(19), 5145–5153. https://doi.org/10.1175/2008jcli2292.1

Hwang, Y.-T., Xie, S.-P., Deser, C., & Kang, S. M. (2017). Connecting tropical climate change with Southern Ocean heat uptake. *Geophysical Research Letters*, *44*(18), 9449–9457. https://doi.org/10.1002/2017gl074972

Ishii, M., Shouji, A., Sugimoto, S., & Matsumoto, T. (2005). Objective analyses of sea-surface temperature and marine meteorological variables for the 20th century using ICOADS and the Kobe collection. *International Journal of Climatology: A Journal of the Royal Meteorological Society*, *25*(7), 865–879. https://doi.org/10.1002/joc.1169

Jeffrey, S., Rotstayn, L., Collier, M., Dravitzki, S., Hamalainen, C., Moeseneder, C., et al. (2013). Australia's CMIP5 submission using the CSIRO Mk3. 6 model. *Australian Meteorological and Oceanographic Journal*, *63*, 1–13. https://doi.org/10.22499/2.6301.001

Jiménez-de-la Cuesta, D., & Mauritsen, T. (2019). Emergent constraints on Earth's transient and equilibrium response to doubled CO_2 from post-1970s global warming. *Nature Geoscience*, *12*(11), 902–905. https://doi.org/10.1038/s41561-019-0463-y

Kang, S. M., Hawcroft, M., Xiang, B., Hwang, Y.-T., Cazes, G., Codron, F., et al. (2019). Extratropical–tropical interaction model intercomparison project (ETIN-MIP): Protocol and initial results. *Bulletin of the American Meteorological Society*, *100*(12), 2589–2606. 10.1175/BAMS-D-18-0301.1

Karnauskas, K. B., Seager, R., Kaplan, A., Kushnir, Y., & Cane, M. A. (2009). Observed strengthening of the zonal sea surface temperature gradient across the equatorial Pacific Ocean. *Journal of Climate*, *22*(16), 4316–4321. https://doi.org/10.1175/2009jcli2936.1

Kay, J., Deser, C., Phillips, A., Mai, A., Hannay, C., Strand, G., et al. (2015). The Community Earth System Model (CESM) large ensemble project: A community resource for studying climate change in the presence of internal climate variability. *Bulletin of the American Meteorological Society*, *96*(8), 1333–1349. https://doi.org/10.1175/bams-d-13-00255.1

Keil, P., Schmidt, H., Stevens, B., & Bao, J. (2021). Variations of tropical lapse rates in climate models and their implications for upper-tropospheric warming. *Journal of Climate*, *34*(24), 9747–9761. https://doi.org/10.1175/JCLI-D-21-0196.1

Kelley, M., Schmidt, G. A., Nazarenko, L. S., Bauer, S. E., Ruedy, R., Russell, G. L., et al. (2020). GISS-E2.1: Configurations and climatology. *Journal of Advances in Modeling Earth Systems*, *12*(8), e2019MS002025. https://doi.org/10.1029/2019ms002025

Kim, H., Kang, S. M., Kay, J. E., & Xie, S.-P. (2022). Subtropical clouds key to Southern Ocean teleconnections to the tropical Pacific. *Proceedings of the National Academy of Sciences*, *119*(34), e2200514119. https://doi.org/10.1073/pnas.2200514119

Kirchmeier-Young, M. C., Zwiers, F. W., & Gillett, N. P. (2017). Attribution of extreme events in Arctic sea ice extent. *Journal of Climate*, *30*(2), 553–571. https://doi.org/10.1175/jcli-d-16-0412.1

Kobayashi, S., Ota, Y., Harada, Y., Ebita, A., Moriya, M., Onoda, H., et al. (2015). The JRA-55 reanalysis: General specifications and basic characteristics. *Journal of the Meteorological Society of Japan. Ser. II*, *93*(1), 5–48. https://doi.org/10.2151/jmsj.2015-001

Kociuba, G., & Power, S. B. (2015). Inability of CMIP5 models to simulate recent strengthening of the Walker circulation: Implications for projections. *Journal of Climate*, *28*(1), 20–35. https://doi.org/10.1175/jcli-d-13-00752.1

Kohyama, T., Hartmann, D. L., & Battisti, D. S. (2017). La Niña–like mean-state response to global warming and potential oceanic roles. *Journal of Climate*, *30*(11), 4207–4225. https://doi.org/10.1175/jcli-d-16-0441.1

Kostov, Y., Ferreira, D., Armour, K. C., & Marshall, J. (2018). Contributions of greenhouse gas forcing and the Southern Annular Mode to historical Southern Ocean surface temperature trends. *Geophysical Research Letters*, *45*(2), 1086–1097. https://doi.org/10.1002/2017gl074964

L'Heureux, M. L., Lee, S., & Lyon, B. (2013). Recent multidecadal strengthening of the Walker circulation across the tropical Pacific. *Nature Climate Change*, *3*(6), 571–576. https://doi.org/10.1038/nclimate1840

Laepple, T., & Huybers, P. (2014). Ocean surface temperature variability: Large model–data differences at decadal and longer periods. *Proceedings of the National Academy of Sciences of the United States of America*, *111*(47), 16682–16687. https://doi.org/10.1073/pnas.1412077111

Ma, S., & Zhou, T. (2016). Robust strengthening and westward shift of the tropical Pacific Walker circulation during 1979–2012: A comparison of 7 sets of reanalysis data and 26 CMIP5 models. *Journal of Climate*, *29*(9), 3097–3118. https://doi.org/10.1175/jcli-d-15-0398.1

Maher, N., Milinski, S., Suarez-Gutierrez, L., Botzet, M., Dobrynin, M., Kornblueh, L., et al. (2019). The Max Planck Institute grand ensemble: Enabling the exploration of climate system variability. *Journal of Advances in Modeling Earth Systems*, *11*(7), 2050–2069. https://doi.org/10.1029/2019MS001639

McGregor, S., Stuecker, M. F., Kajtar, J. B., England, M. H., & Collins, M. (2018). Model tropical Atlantic biases underpin diminished Pacific decadal variability. *Nature Climate Change*, *8*(6), 493–498. https://doi.org/10.1038/s41558-018-0163-4

Meehl, G. A., & Washington, W. M. (1996). El Niño-like climate change in a model with increased atmospheric CO_2 concentrations. *Nature*, *382*(6586), 56–60. https://doi.org/10.1038/382056a0

Neelin, J. D., Battisti, D. S., Hirst, A. C., Jin, F.-F., Wakata, Y., Yamagata, T., & Zebiak, S. E. (1998). ENSO theory. *Journal of Geophysical Research*, *103*(C7), 14261–14290. https://doi.org/10.1029/97jc03424

Nijsse, F. J., Cox, P. M., & Williamson, M. S. (2020). Emergent constraints on transient climate response (TCR) and equilibrium climate sensitivity (ECS) from historical warming in CMIP5 and CMIP6 models. *Earth System Dynamics*, *11*(3), 737–750. https://doi.org/10.5194/esd-11-737-2020

Olonscheck, D., Rugenstein, M., & Marotzke, J. (2020). Broad consistency between observed and simulated trends in sea surface temperature patterns. *Geophysical Research Letters*, *47*(10), e2019GL086773. https://doi.org/10.1029/2019gl086773

Parsons, L. A., Brennan, M. K., Wills, R. C. J., & Proistosescu, C. (2020). Magnitudes and spatial patterns of interdecadal temperature variability in CMIP6. *Geophysical Research Letters*, *47*(7), e2019GL086588. https://doi.org/10.1029/2019gl086588

Pauling, A. G., Bitz, C. M., Smith, I. J., & Langhorne, P. J. (2016). The response of the Southern Ocean and Antarctic sea ice to freshwater from ice shelves in an Earth system model. *Journal of Climate*, *29*(5), 1655–1672. https://doi.org/10.1175/jcli-d-15-0501.1

Purich, A., England, M. H., Cai, W., Sullivan, A., & Durack, P. J. (2018). Impacts of broad-scale surface freshening of the Southern Ocean in a coupled climate model. *Journal of Climate*, *31*(7), 2613–2632. https://doi.org/10.1175/jcli-d-17-0092.1

Qin, M., Dai, A., & Hua, W. (2020). Aerosol-forced multidecadal variations across all ocean basins in models and observations since 1920. *Science Advances*, *6*(29), eabb0425. https://doi.org/10.1126/sciadv.abb0425

Rodgers, K. B., Lee, S.-S., Rosenbloom, N., Timmermann, A., Danabasoglu, G., Deser, C., et al. (2021). Ubiquity of human-induced changes in climate variability. *Earth System Dynamics Discussions*, *12*(4), 1–22. https://doi.org/10.5194/esd-12-1393-2021

Rodgers, K. B., Lin, J., & Frölicher, T. L. (2015). Emergence of multiple ocean ecosystem drivers in a large ensemble suite with an Earth system model. *Biogeosciences*, *12*(11), 3301–3320. https://doi.org/10.5194/bg-12-3301-2015

Samanta, D., Karnauskas, K. B., Goodkin, N. F., Coats, S., Smerdon, J. E., & Zhang, L. (2018). Coupled model biases breed spurious low-frequency variability in the tropical Pacific Ocean. *Geophysical Research Letters*, *45*(19), 10–609. https://doi.org/10.1029/2018gl079455

Sardeshmukh, P. D., & Hoskins, B. J. (1988). The generation of global rotational flow by steady idealized tropical divergence. *Journal of the Atmospheric Sciences*, *45*(7), 1228–1251. https://doi.org/10.1175/1520-0469(1988)045<1228:tggrf>2.0.co;2

Schneider, D. P., & Deser, C. (2018). Tropically driven and externally forced patterns of Antarctic sea ice change: Reconciling observed and modeled trends. *Climate Dynamics*, *50*(11), 4599–4618. https://doi.org/10.1007/s00382-017-3893-5

Schneider, T., & Griffies, S. M. (1999). A conceptual framework for predictability studies. *Journal of Climate*, *12*(10), 3133–3155. https://doi.org/10.1175/1520-0442(1999)012<3133:acffps>2.0.co;2

Seager, R., Cane, M., Henderson, N., Lee, D.-E., Abernathey, R., & Zhang, H. (2019). Strengthening tropical Pacific zonal sea surface temperature gradient consistent with rising greenhouse gases. *Nature Climate Change*, *9*(7), 517–522. https://doi.org/10.1038/s41558-019-0505-x

Seager, R., Henderson, N., & Cane, M. (2022). Persistent discrepancies between observed and modeled trends in the tropical Pacific Ocean. *Journal of Climate*, *35*(14), 1–41. https://doi.org/10.1175/JCLI-D-21-0648.1

Shi, J.-R., Kwon, Y.-O., & Wijffels, S. E. (2022). Two distinct modes of climate responses to the anthropogenic aerosol forcing changes. *Journal of Climate*, *35*(11), 3445–3457. https://doi.org/10.1175/jcli-d-21-0656.1

Smith, D. M., Booth, B. B., Dunstone, N. J., Eade, R., Hermanson, L., Jones, G. S., et al. (2016). Role of volcanic and anthropogenic aerosols in the recent global surface warming slowdown. *Nature Climate Change*, *6*(10), 936–940. https://doi.org/10.1038/nclimate3058

Sohn, B.-J., Lee, S., Chung, E.-S., & Song, H.-J. (2016). The role of the dry static stability for the recent change in the Pacific Walker circulation. *Journal of Climate*, *29*(8), 2765–2779. https://doi.org/10.1175/jcli-d-15-0374.1

Solomon, A., & Newman, M. (2012). Reconciling disparate twentieth-century Indo-Pacific ocean temperature trends in the instrumental record. *Nature Climate Change*, *2*(9), 691–699. https://doi.org/10.1038/nclimate1591

Suarez-Gutierrez, L., Milinski, S., & Maher, N. (2021). Exploiting large ensembles for a better yet simpler climate model evaluation. *Climate Dynamics*, *57*(9), 2557–2580. https://doi.org/10.1007/s00382-021-05821-w

Sun, L., Alexander, M., & Deser, C. (2018). Evolution of the global coupled climate response to Arctic sea ice loss during 1990–2090 and its contribution to climate change. *Journal of Climate*, *31*(19), 7823–7843. https://doi.org/10.1175/jcli-d-18-0134.1

Swain, D. L., Tsiang, M., Haugen, M., Singh, D., Charland, A., Rajaratnam, B., & Diffenbaugh, N. S. (2014). The extraordinary California drought of 2013/2014: Character, context, and the role of climate change. *Bulletin of the American Meteorological Society*, *95*(9), S3.

Swart, N. C., Cole, J. N., Kharin, V. V., Lazare, M., Scinocca, J. F., Gillett, N. P., et al. (2019). The Canadian Earth System Model version 5 (CanESM5.0.3). *Geoscientific Model Development*, *12*(11), 4823–4873. https://doi.org/10.5194/gmd-12-4823-2019

Tatebe, H., Ogura, T., Nitta, T., Komuro, Y., Ogochi, K., Takemura, T., et al. (2019). Description and basic evaluation of simulated mean state, internal variability, and climate sensitivity in MIROC6. *Geoscientific Model Development*, *12*(7), 2727–2765. https://doi.org/10.5194/gmd-12-2727-2019

Taylor, K. E., Stouffer, R. J., & Meehl, G. A. (2012). An overview of CMIP5 and the experiment design. *Bulletin of the American Meteorological Society*, *93*(4), 485–498. https://doi.org/10.1175/BAMS-D-11-00094.1

Thompson, D. W., Solomon, S., Kushner, P. J., England, M. H., Grise, K. M., & Karoly, D. J. (2011). Signatures of the Antarctic ozone hole in Southern Hemisphere surface climate change. *Nature Geoscience*, *4*(11), 741–749. https://doi.org/10.1038/ngeo1296

Tierney, J. E., Haywood, A. M., Feng, R., Bhattacharya, T., & Otto-Bliesner, B. L. (2019). Pliocene warmth consistent with greenhouse gas forcing. *Geophysical Research Letters*, *46*(15), 9136–9144. https://doi.org/10.1029/2019gl083802

Ting, M., Kushnir, Y., Seager, R., & Li, C. (2009). Forced and internal twentieth-century SST trends in the North Atlantic. *Journal of Climate*, *22*(6), 1469–1481. https://doi.org/10.1175/2008jcli2561.1

Tokarska, K. B., Stolpe, M. B., Sippel, S., Fischer, E. M., Smith, C. J., Lehner, F., & Knutti, R. (2020). Past warming trend constrains future warming in CMIP6 models. *Science Advances*, *6*(12), eaaz9549. https://doi.org/10.1126/sciadv.aaz9549

Tokinaga, H., Xie, S.-P., Deser, C., Kosaka, Y., & Okumura, Y. M. (2012). Slowdown of the Walker circulation driven by tropical Indo-Pacific warming. *Nature*, *491*(7424), 439–443. https://doi.org/10.1038/nature11576

Trenberth, K. E., & Fasullo, J. T. (2013). An apparent hiatus in global warming? *Earth's Future*, *1*(1), 19–32. https://doi.org/10.1002/2013ef000165

Turner, J., & Overland, J. (2009). Contrasting climate change in the two polar regions. *Polar Research*, *28*(2), 146–164. https://doi.org/10.1111/j.1751-8369.2009.00128.x

Vecchi, G. A., Soden, B. J., Wittenberg, A. T., Held, I. M., Leetmaa, A., & Harrison, M. J. (2006). Weakening of tropical Pacific atmospheric circulation due to anthropogenic forcing. *Nature*, *441*(7089), 73–76. https://doi.org/10.1038/nature04744

Voldoire, A., Saint-Martin, D., Sénési, S., Decharme, B., Alias, A., Chevallier, M., et al. (2019). Evaluation of CMIP6 deck experiments with CNRM-CM6-1. *Journal of Advances in Modeling Earth Systems*, *11*(7), 2177–2213. https://doi.org/10.1029/2019ms001683

Waskom, M. L. (2021). Seaborn: Statistical data visualization. *Journal of Open Source Software*, *6*(60), 3021. https://doi.org/10.21105/joss.03021

Watanabe, M., Dufresne, J.-L., Kosaka, Y., Mauritsen, T., & Tatebe, H. (2021). Enhanced warming constrained by past trends in equatorial Pacific sea surface temperature gradient. *Nature Climate Change*, *11*(1), 33–37. https://doi.org/10.1038/s41558-020-00933-3

Wills, R. C. J., Armour, K. C., Battisti, D. S., Proistosescu, C., & Parsons, L. A. (2021). Slow modes of global temperature variability and their impact on climate sensitivity estimates. *Journal of Climate*, *34*(21), 8717–8738. https://doi.org/10.1175/jcli-d-20-1013.1

Wills, R. C. J., Battisti, D. S., Armour, K. C., Schneider, T., & Deser, C. (2020). Pattern recognition methods to separate forced responses from internal variability in climate model ensembles and observations. *Journal of Climate*, *33*(20), 8693–8719. https://doi.org/10.1175/jcli-d-19-0855.1

Wyser, K., Koenigk, T., Fladrich, U., Fuentes-Franco, R., Karami, M. P., & Kruschke, T. (2021). The SMHI large ensemble (SMHI-LENS) with EC-Earth3.3.1. *Geoscientific Model Development*, *14*(7), 4781–4796. https://doi.org/10.5194/gmd-14-4781-2021

Zhang, L., Delworth, T. L., Cooke, W., & Yang, X. (2019). Natural variability of Southern Ocean convection as a driver of observed climate trends. *Nature Climate Change*, *9*(1), 59–65. https://doi.org/10.1038/s41558-018-0350-3

Zhang, L., Delworth, T. L., & Jia, L. (2017). Diagnosis of decadal predictability of Southern Ocean sea surface temperature in the GFDL CM2.1 model. *Journal of Climate*, *30*(16), 6309–6328. https://doi.org/10.1175/jcli-d-16-0537.1

Zhang, L., & Karnauskas, K. B. (2017). The role of tropical interbasin SST gradients in forcing Walker circulation trends. *Journal of Climate*, *30*(2), 499–508. https://doi.org/10.1175/jcli-d-16-0349.1

Zhang, X., Deser, C., & Sun, L. (2021). Is there a tropical response to recent observed Southern Ocean cooling? *Geophysical Research Letters*, *48*(5), e2020GL091235. https://doi.org/10.1029/2020gl091235

Zhao, X., & Allen, R. J. (2019). Strengthening of the Walker circulation in recent decades and the role of natural sea surface temperature variability. *Environmental Research Communications*, *1*(2), 021003. https://doi.org/10.1088/2515-7620/ab0dab

Zhou, C., Zelinka, M. D., & Klein, S. A. (2016). Impact of decadal cloud variations on the Earth's energy budget. *Nature Geoscience*, *9*(12), 871–874. https://doi.org/10.1038/ngeo2828

Ziehn, T., Chamberlain, M. A., Law, R. M., Lenton, A., Bodman, R. W., Dix, M., et al. (2020). The Australian Earth system model: ACCESS-ESM1.5. *Journal of Southern Hemisphere Earth Systems Science*, *70*(1), 193–214. https://doi.org/10.1071/es19035